ESTIMATING POROSITY AND WATER SATURATION FROM SEISMIC/ACOUSTIC SIGNALS: A CORRECTION ON THE EFFECT OF SHALINESS

by
Bambang Widarsono and **Fakhriyadi Saptono**

ABSTRACT

The presence of shale in sedimentary rocks tends to introduce complexity in any formation evaluation activities. This is also the case when efforts are spent in establishing a method that enables analysts to estimate porosity and water saturation from seismic survey. The method, which is a combination of laboratory measurement, mathematical modeling (Gassmann model), and log interpretation, has been proposed earlier. However, scatter and inconsistencies in compressional wave velocities with regard to porosity and water saturation was often encountered when it came to apply the method. This certainly affects the reliability of acoustic velocity data that is needed by the method. Therefore it is the objective of the work presented in this paper to modify the method with an emphasis at accommodating the effect of shaliness.

The effect of shaliness, as well as variation in matrix density, tends to complicate the relations between acoustic velocities, acoustic impedance, and Poisson ratio on one side and porosity and water saturation on the other side. This poses difficulties to one part of the porosity-water saturation estimation method, in which it relies almost entirely on consistency between the above-mentioned rock and acoustic properties. This certainly reduces the reliability of the method. Therefore, the weight of this work lies on recognizing the effect of shaliness through division of the rock and acoustic properties following a set of ranges in shale fraction and matrix density. It was hoped that the division would reduce the degree of scatter and inconsistencies mentioned earlier.

To facilitate the investigation, two sets of core samples taken from a sandstone oil reservoir in Central Sumatra and a limestone reservoir in Natuna. Upon application of the method, the division proves itself encouraging when applied on the Central Sumatra sandstone, but does not deliver a satisfactory outcome when applied on the Natuna limestone. This is probably due to the large influence exerted by the limestone's pore configuration. Nevertheless, the work has provided the required modification on the existing method, hence making it more reliable. Another valuable result is the underlining of the postulate stating that any presence of shale has to be handled separately if accurate results are to be accomplished.

I. INTRODUCTION

The distribution of porosity and water saturation throughout reservoir body is considered as an important factor in the effort to develop reservoir models. Various endeavors have been devoted to establishing reliable methods for serving the purpose. Developments in recent years have witnessed the increasing attention on the possibility of utilizing seismic survey data (especially the 3D) for supporting reservoir characterization. This includes estimating the distribution of inter-well porosity and water saturation.

The interest on understanding the relations between acoustic properties and rock petrophysical properties has always been in existence since 1950s. Early investigations by King (1966), Gregory (1976), and Domenico (1976) had shown that there are relationships between acoustic velocities and water saturation, as suggested by some acoustic propagation theories such as those proposed by Gasmann (1951) and Biot (1956). However, the results were received with skepticism when it came to a suggestion that they be applied on seismic data. Recently, rapid developments in seismic processing technology have revived the hope to use seismic data for determining porosity and water saturation throughout reservoir. For instance, King (1996a, 1996b) optimistically discussed the feasibility of applying the relationship on the concept of 4D seismic monitoring. In implementing such concept further understanding over relationship between acoustic velocities and rock properties is necessary.

Widarsono and Saptono (1997) in their laboratory works proposed a procedure for preparing laboratory data of acoustic measurement on reservoir rocks for the purpose of seismic-guided reservoir characterization. The procedure was refined further in Widarsono and Saptono (1999). The method, in the procedure, is a combination between mathematical modeling (based on Gassmann, 1951) of acoustic velocities on shale-free (clean) rock samples, well-log interpretation, and laboratory acoustic measurements on cores at various water saturations. In applying the method, problems were encountered in the form of

inconsistencies between compressional velocities, porosities, and water saturation. It was strongly suspected that shaliness and variation in rock density are the main causes. It is therefore the purpose of the works presented in this paper to provide a further understanding regarding the matter. It is hoped that an improved understanding will provide better procedure that can provide more accurate models for supporting seismic-guided reservoir characterization.

II. THE EFFECT OF SHALINESS ON ACOUSTIC PROPERTIES – A PERSPECTIVE

Acoustic propagation properties of elastic media, as described in various textbooks (e.g. Fjaer et al, 1992), are relatively simple when compared to media that bear pores and cracks. Various theories, such as one proposed by Gassmann (1951), Biot (1956), and Kuster and Tokzos (1974), include more complications by incorporating rock frame, pore-fluid, and rock-grain compressibility into the velocity equations. It is obvious that the presence of shale affects the matrix properties such as dry bulk modulus and rock frame bulk modulus, and consequently also the acoustic transit time (e.g. t and t), hence velocities (e.g. V and V). Such alteration also results in altered mechanical properties such as Poisson ratio, bulk modulus, and Young's modulus, as can easily shown by the theory of elasticity (or acoustic propagation in elastic medium) of porous medium.

In general, the presence of shale certainly complicates matters in reservoir characterization. Various studies have unrevealed the complexity between various rock properties and signals used in surveying them when the cases include shale presence. As shown by Hartley (1981), for example, porosity predictions from any empirical relations using acoustic-wave transit time are worse for shaly sands. Despite the efforts that have been spent on them, effects of shale on acoustic velocities are not very well understood, and therefore difficult to account for.

The shale-related complexities can be apprehended through the different ways by which shale is defined. Grim (1968), with excellence, pointed out that there are differences in the way engineers and geologists define shale. To most engineers shale is regarded similar to soil except that the term is applied to material that is slightly harder and is definitely argillaceous. Some also define shale as formed by any silt- and clay-size materials. On the other hand, to most geologist shale is a fine-grained, earthy, sedimentary rock with a distinct laminated character due to a general parallel arrangement of flake-shaped or elongate particles. Occasionally, however, natural materials are called shale with little regard to composition, often with very little clay-mineral component. Regardless the differences, these are to emphasize the wide range of minerals that could form shale, including quartz and carbonates. This is indeed the reason behind the difficulties in establishing a typical and specific acoustic characteristics for shale. This is best reflected by the large range of compressional wave velocity (V_p) of 7,000 – 17,000 ft/sec for various shale, compared to sandstones (9,000 – 16,000 ft/sec) and limestones (13,000 – 18,500 ft/sec), as shown by Timur (1987).

Various investigators have also reported different findings. Some reported that the presence of shale affects the acoustic wave velocities significantly. For instance Koerperich (1980) showed that the presence of shale in Bill Stribling sandstone tends to increase the V while the reverse is true for a similar presence in Bilf Stribling limestone. There were also investigators who observed different alteration on acoustic velocities caused by different shale structures (e.g. Minear, 1982). All these findings enforce the prevailing presumption that the presence of shale has to be treated carefully, and by no means be generalized in its influence.

III. CASE HISTORY - THE NEED TO INCLUDE THE EFFECT OF SHALINESS

As mentioned earlier, Widarsono and Saptono (1997) proposed a procedure to prepare data of laboratory acoustic measurement on rock samples at various water saturation and overburden pressure. In general, the procedure consists of several main steps:

1. Measurement of compressional (V_p, example: Figure 1a), as well as shear wave velocities, V_s, at various arranged water saturation and overburden pressure. The corresponding Poisson ratio are calculated using the two velocities (example: Figure 1b).
2. Application of mathematical model (see Appendix) on the data, creating a relationship (crossplot) between V_p, Poisson ratio, porosity and water saturation (example: Figure 2).
3. Conversion of the crossplot to *in situ* (i.e. reservoir) condition using a plot between V from the validated model ($V_{p,model}$) versus V_p from well-log interpretation results ($V_{p,log}$), for the same porosity and water saturation values taken from log interpretation results. An example of the plot is presented in Figure 3. Note the scatter shown by the data. The mentioned conversion is actually needed to calibrate the crossplot, which is itself basically developed in laboratory condition.
4. Remodeling of the converted V_p and other properties, and establishing a new crossplot similar to the one presented in Figure 2.
5. Model validation using data from well-log. Using the

Gassmann model and the theory of elasticity for brittle material (e.g. presented by Timur, 1987) the validation is made under tolerance of porosity of 2 % (porosity unit) and Poisson ratio of 0.002. The calculated $S_{w,model}$ values are compared to their corresponding $S_{w,log}$ used as reference.

6. Assuming the lithology model is valid throughout the relevant reservoir, the crossplot is considered ready for estimating porosity and water saturation whenever V_p and Poisson ratio data from seismic survey has been made available.

The process of modeling and establishment of the crossplot in Figure 2 is under an assumption that the reservoir rocks are clean (shale-free) in nature. However, this is not always the case for reservoir rocks. It is a rule rather than an exception that shale is usualy present in reservoir rocks. This is best reflected by the scatter shown by the plot in Figure 3, even though variation in lithology is also expected to be responsible.

To observe and take into acount the effect of shaliness, a set of sandstone cores from a producing well in Central Sumatra (oil) was taken for acoustic measurements in laboratory. In addition, a set of reef limestone cores from Natuna (gas) was also taken for measurement. Following the standard arrangement for the measurement, data was obtained and processed using the procedure described above.

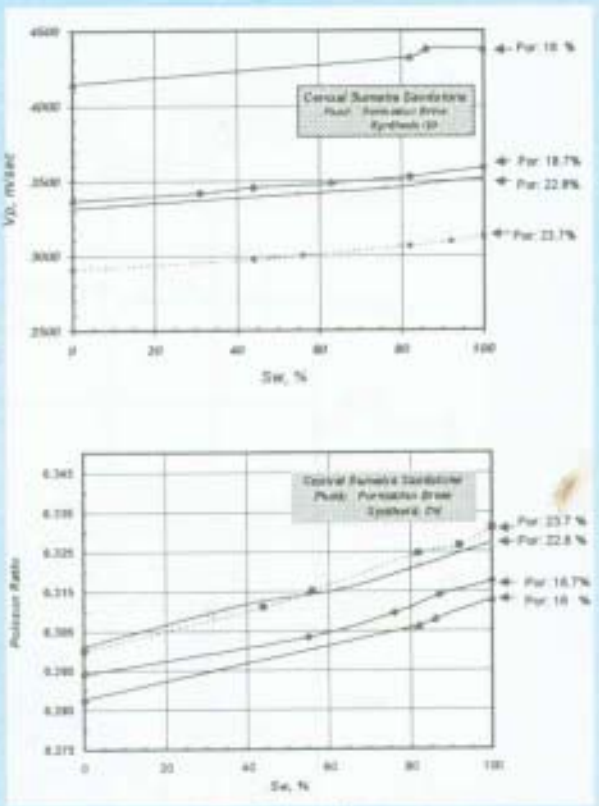

Figure 1
Example of acoustic measurement on cores (Central Sumatra sandstone)

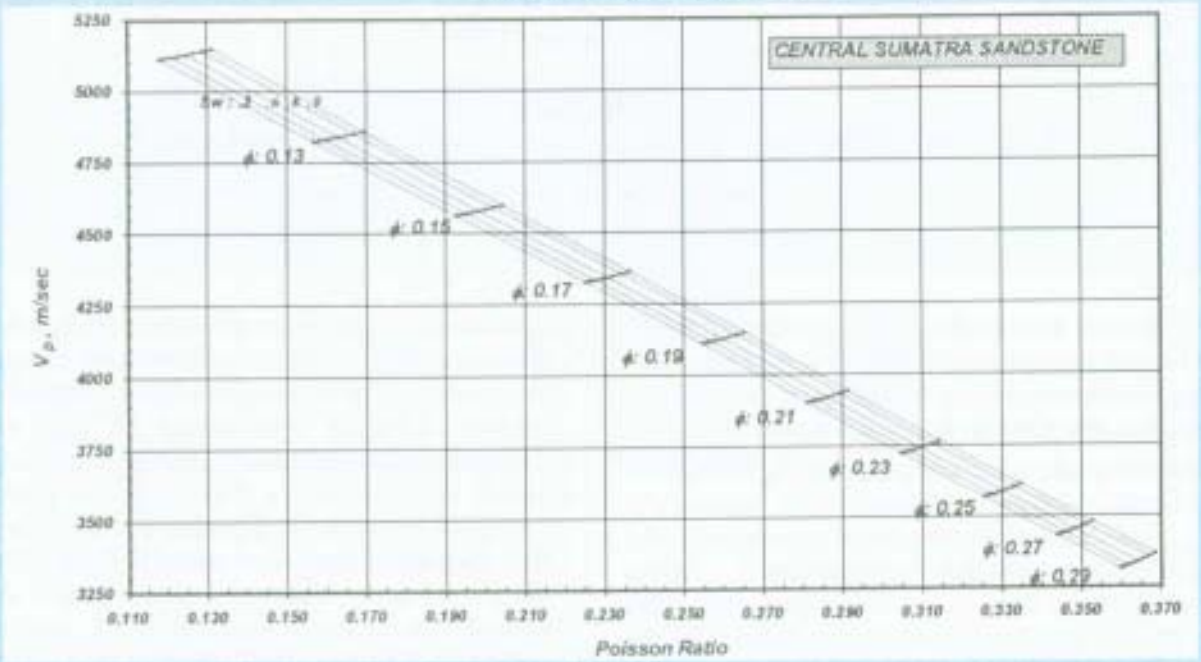

Figure2
Crossplot as the result of mathematical modeling for the Central Sumatra Sandstone (laboratory condition)

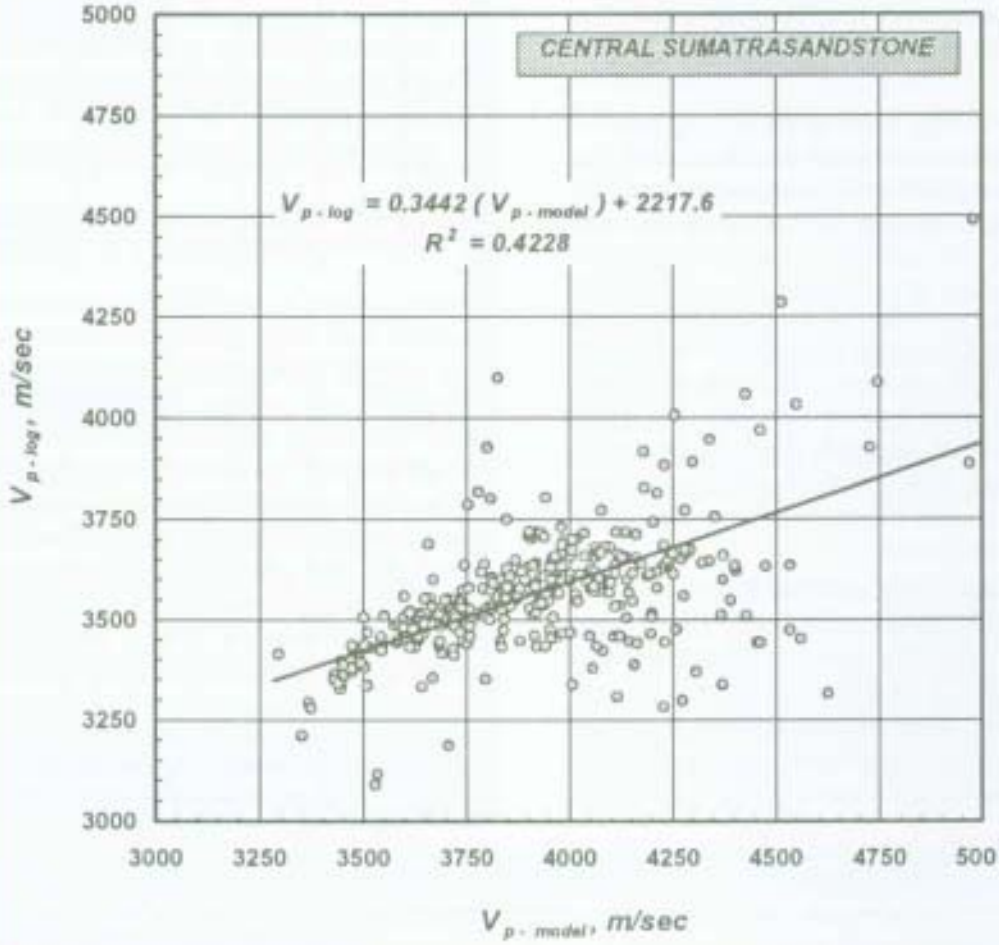

Figure 3
$V_{p\text{-model}}$ vs $V_{p\text{-log}}$ used for conversion/calibration into in situ condition and without acomodating the effect of shaliness
(Central Sumatra Sandstone)

Figure 1 presents an example of the measurement results for the Central Sumatra cores whereas Figure 2 represents modeling result (crossplot) on the laboratory data. Similar treatment was also given to the limestone data.

Using the results of log interpretation (Figures 4 and 5 for the Central Sumatra and Natuna wells, respectively) the $V_{p,model}$ values that represent pairs of porosity and water saturation values receive their corresponding $V_{p,log}$ values that represent the same pairs of porosity and water saturation. The plot between the two velocities (for the Central Sumatra sandstone) is presented in Figure 3. Using the expression from linear-regression the relationship shown in Figure 2 is then converted to a similar crossplot but considered valid for *in situ* condition (Figure 6a for Central Sumatra sandstone). After establishing the crossplot for *in situ* condition, for the purpose of model validation, water saturation values from model ($S_{w,model}$) and their corresponding water saturation values from log ($S_{w,log}$), having the same values of porosity, are plotted. The "validated" crossplot is presented in Figure 6a, whereas the validation process is presented in Figures 6b through 6d. Following the scheme presented in step 5 above it is obvious that the scatter shown by the S_w plot is virtualy intolerable. The "validated" crossplot shown in Figure 6a is therefore actually not valid. Similar process has also been performed for the Natuna limestone.

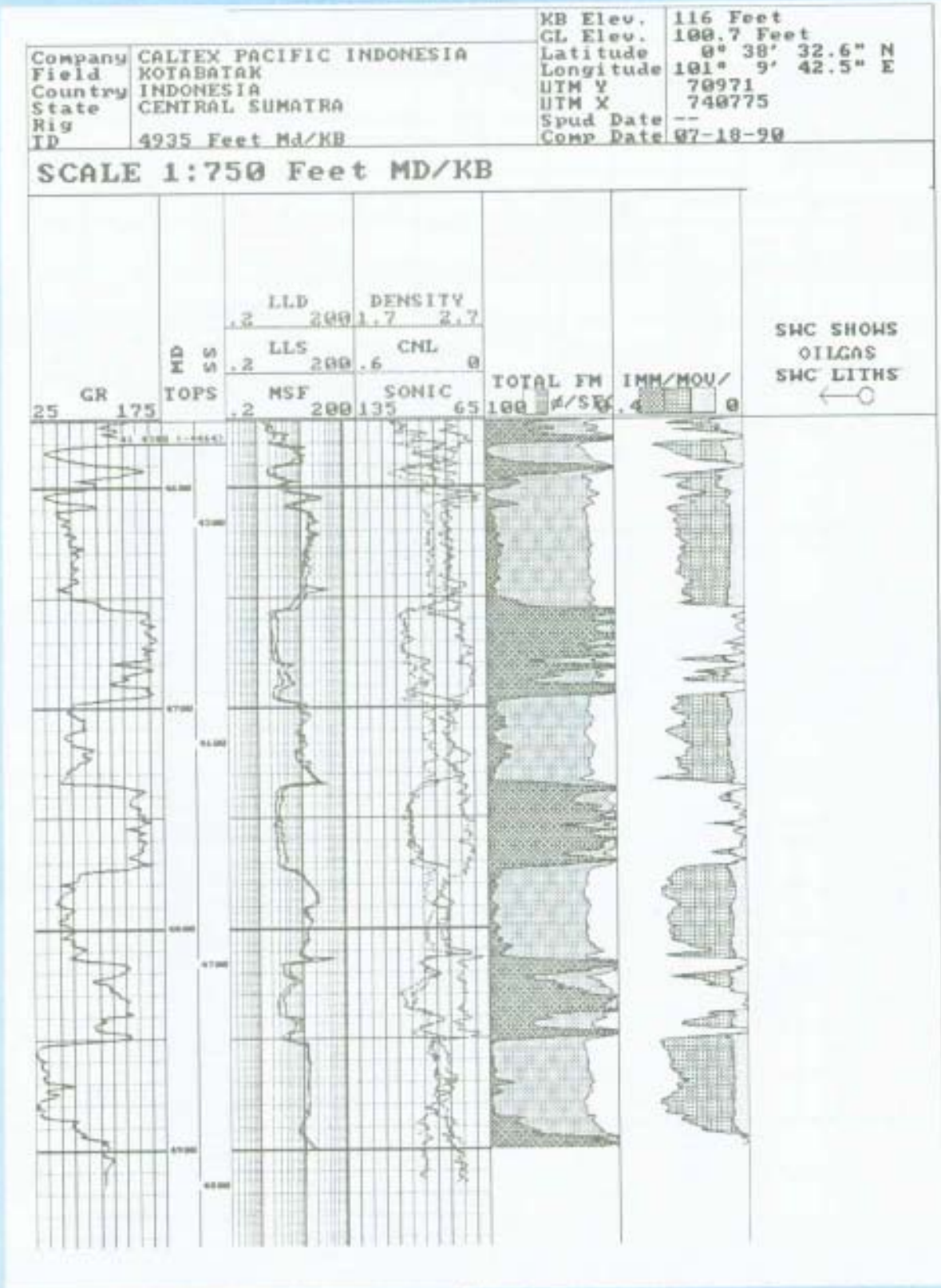

Figure 4
Log interpretation result for the Central Sumatra well

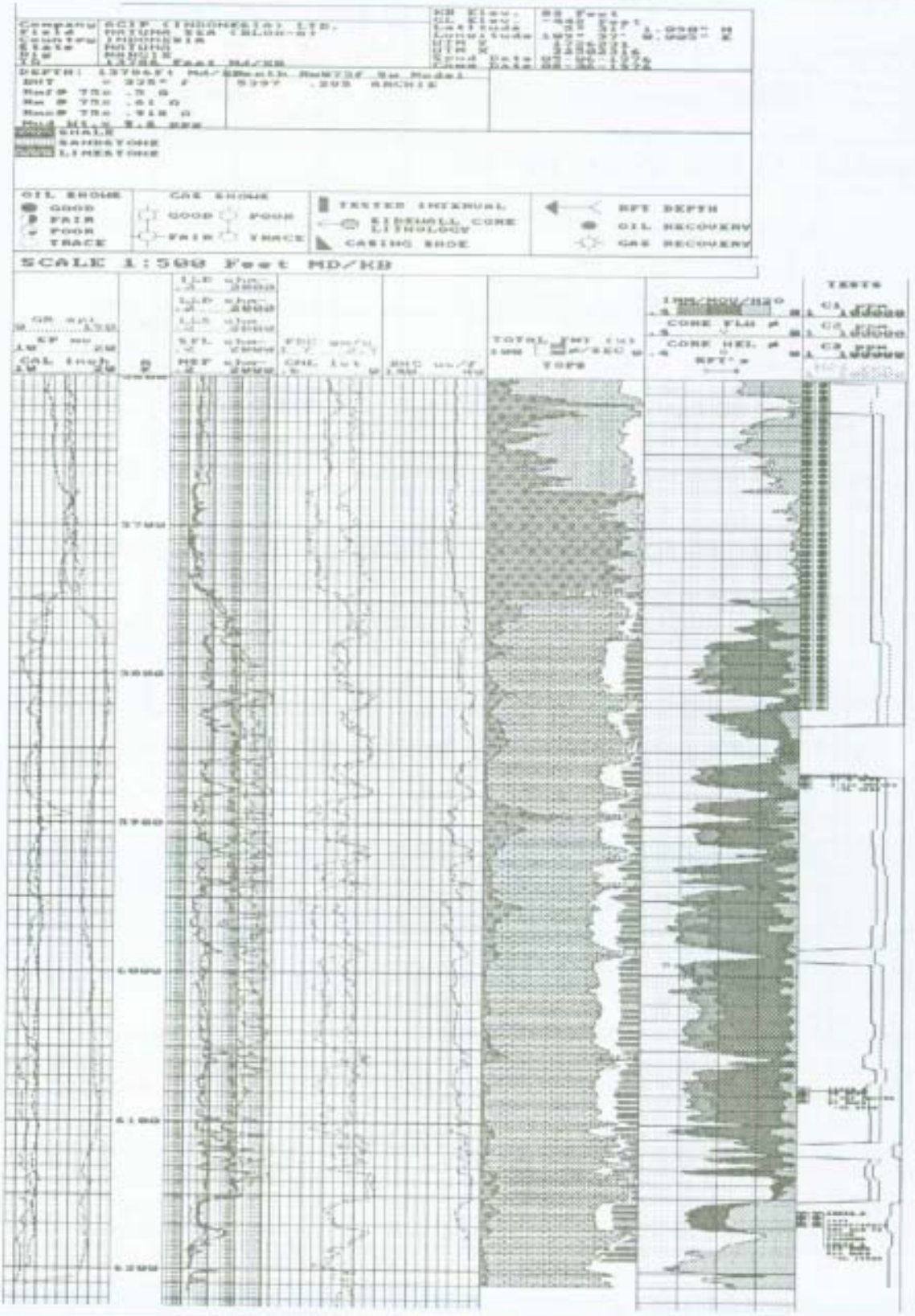

Figure 5
Log interpretation result for the Natuna well

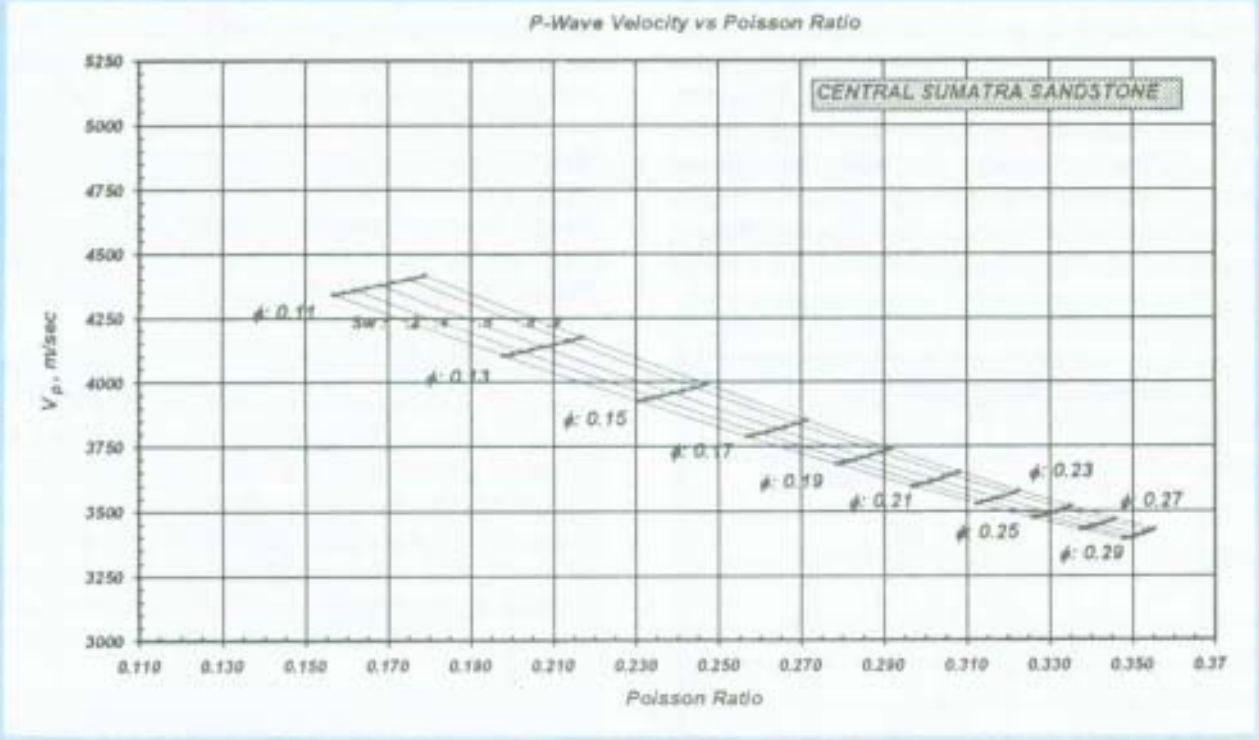

Figure 6a
An example of the resulting crossplots
(in situ condition) for the Central Sumatra sandstone and without acomodating effect of sliness

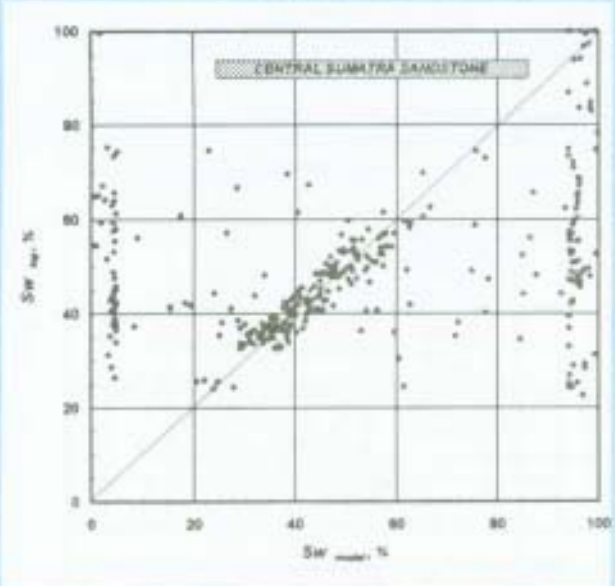

Figure 6b
Model validation through comparison of Poisson Ratio values, without acomodating the effect of shaliness (Central Sumatra sandstone)

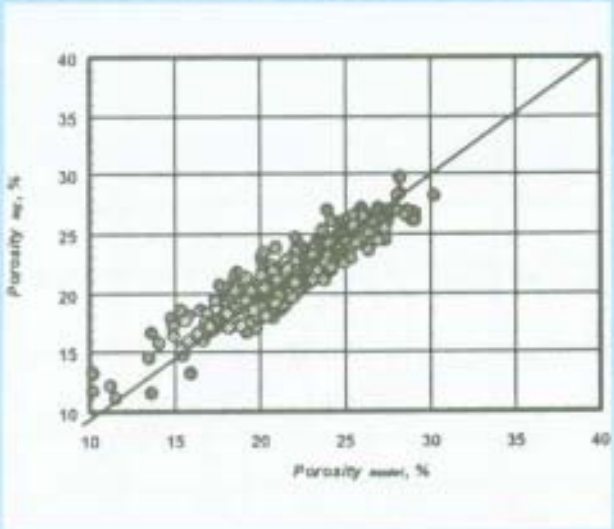

Figure 6c
Model Validation through comparison of Porosity, without acomodating the effect of shaliness
(Central Sumatra sandstone)

The scatter in Figures 3 and 6b certainly reduces the reliability of the crossplot (Figure 6a). Considering the relative ease to match log porosity using the model (Figure 6c), it is obvious that the scatter shown by the S plot is influenced by minerals in the rock matrix. There are, basically, two causes that probably inflict this occurrence, namely variation in lithology (including density) and variation in shale content (shaliness). These two factors were indeed not taken into consideration. By acknowledging the respective influence of the two factors it is hoped that the degree of scatter can be reduced.

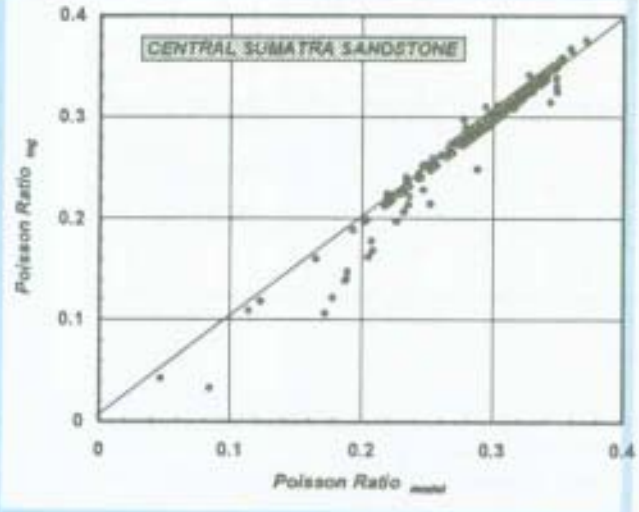

Figure 6d
Model validation through comparison of Poisson Ratio values, without acomodating the effect of shaliness (Central Sumatra sandstone)

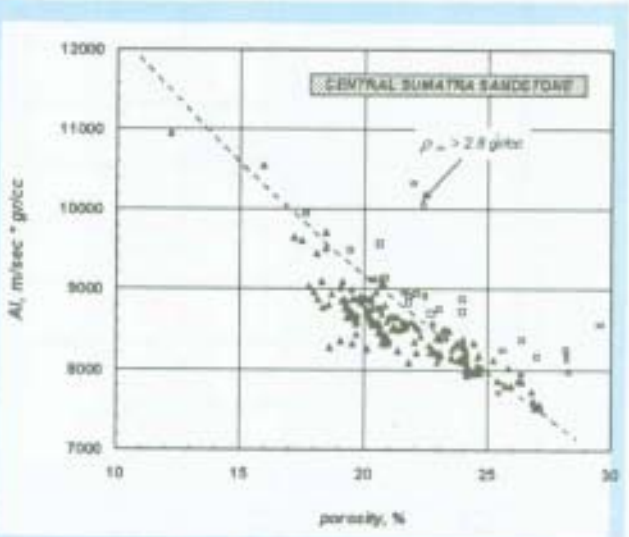

Figure 7
Division based on matrix density (Central Sumatra sandstone)

IV. CONSIDERATION OVER SHALINESS AND VARIATION IN ROCK MATRIX DENSITY

The first step in distinguishing the effect of shaliness and variation in rock density is to create division of relation between V_p and porosity based on differences in matrix density, hence analyzing the first factor. Both V and porosity are taken from log interpretation results whereas the matrix density (r_m) is determined through a rearrangement on.

$$\rho_b = \rho_m(1-\phi) + \phi S_w \rho_w + \phi(1-S_w)\rho_{HC} \qquad (1)$$

where r_b, r_w, and r_{HC} are respectively densities of rock (bulk density), water, and hydrocarbon. Note that r_b is from density log whereas porosity (f) and water saturation (S_w) are from log interpretation result. In order to make the distinction easier, the V_p is expressed in the form of *acoustic impedance* (AI = V x r). The use of acoustic impedance is also considered advantageous considering the ease to produce from seismic survey. The plot is presented in Figure 7.

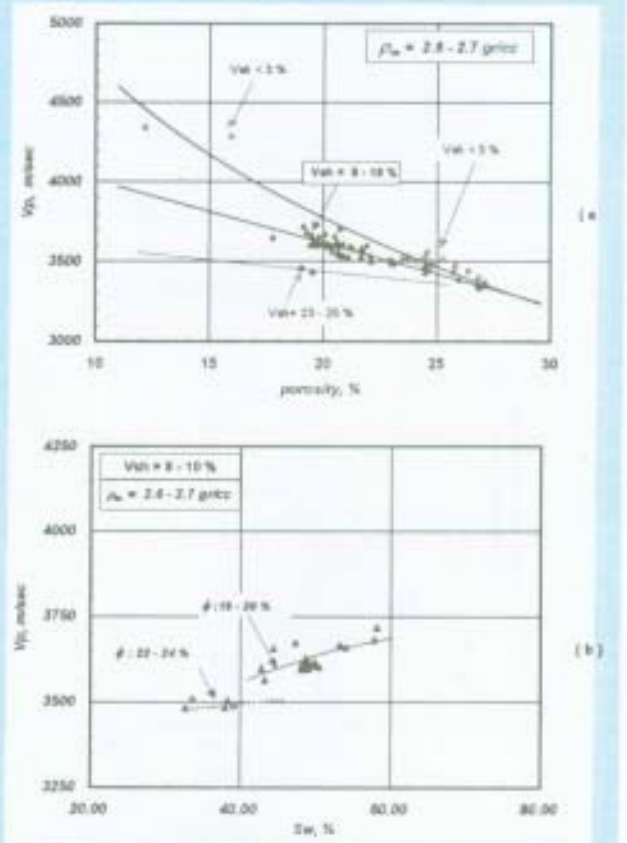

Figure 8
Division based on shale fraction (Central Sumatra sandstone).

The plot for the Central Sumatra sandstone shows that most data are represented by matrix densities between 2.6 and 2.7 gr/cc. Due to their limited number, most of data points representing values outside this range are excluded from the plot. The establishment of the predominant matrix density range is likely to reduce significantly the some of the scatter (as shown by V_p plot in Figure 3) possibly raised by uncertainty in matrix density. Although the matrix density range can still be considered wide the variation of matrix density as a scattering factor has been limited. More thorough division in matrix density range needs to be performed in the future.

Attention is now devoted to the second factor, shaliness. In a manner similar to the observation on the effect of matrix density, the effect of shaliness is observed through a plot between V_p and porosity values taken from log interpretation result (Figure 8a), for data points that are represented by matrix density values within the range of 2.6 – 2.7 gr/cc. The most striking evidence shown by the plot is the relatively obvious grouping among data presenting four ranges of shale fraction (V_{sh}) with three most representative curves. Notice the convergence shown by the three curves indicating the

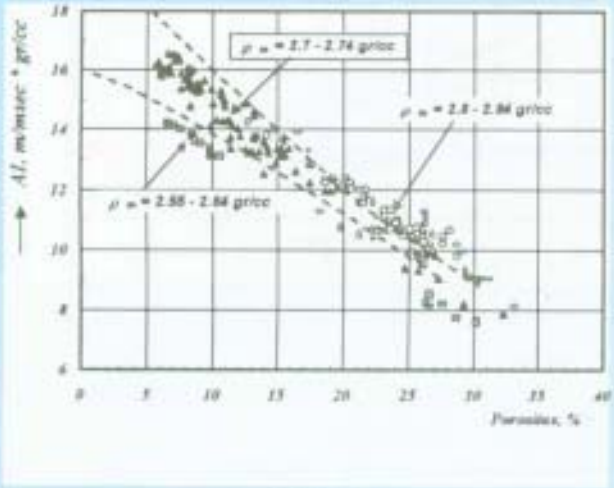

Figure 9
Division based on matrix density
(Natuna limestone)

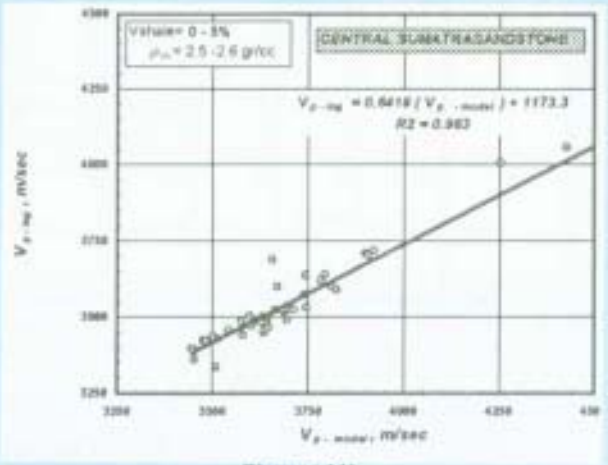

Figure 11b
Vp-model vs Vp-log, used for conversion/calibration into in situ condition after acomodating the effect of shaliness. Vshale=0 - 5 %, rm= 2.5 - 2.6 gr/cc
(Central Sumatra Sandstone)

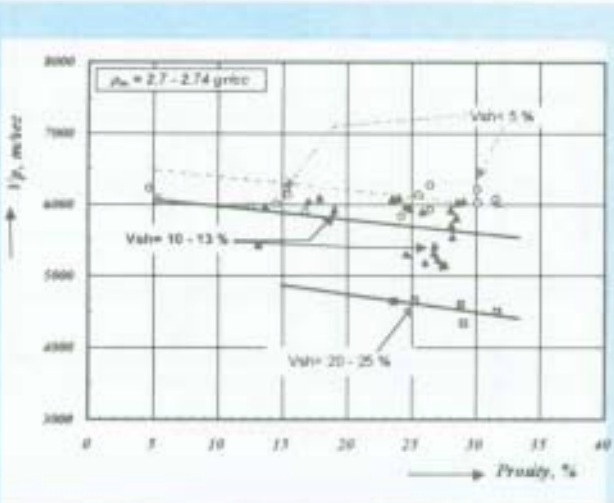

Figure 10
Division based on shale fraction
(Natuna limestone)

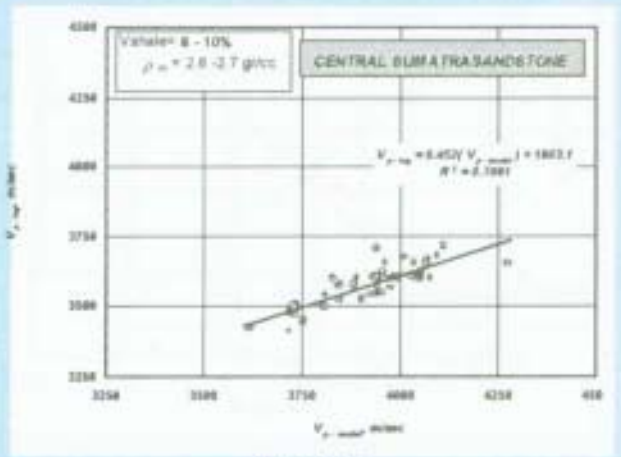

Figure 11a
Vp-model vs Vp-log, used for conversion/calibration into in situ condition after acomodating the effect of shaliness. Vshale= 8 - 10 %, rm= 2.6 - 2.7 gr/cc
(Central Sumatra Sandstone).

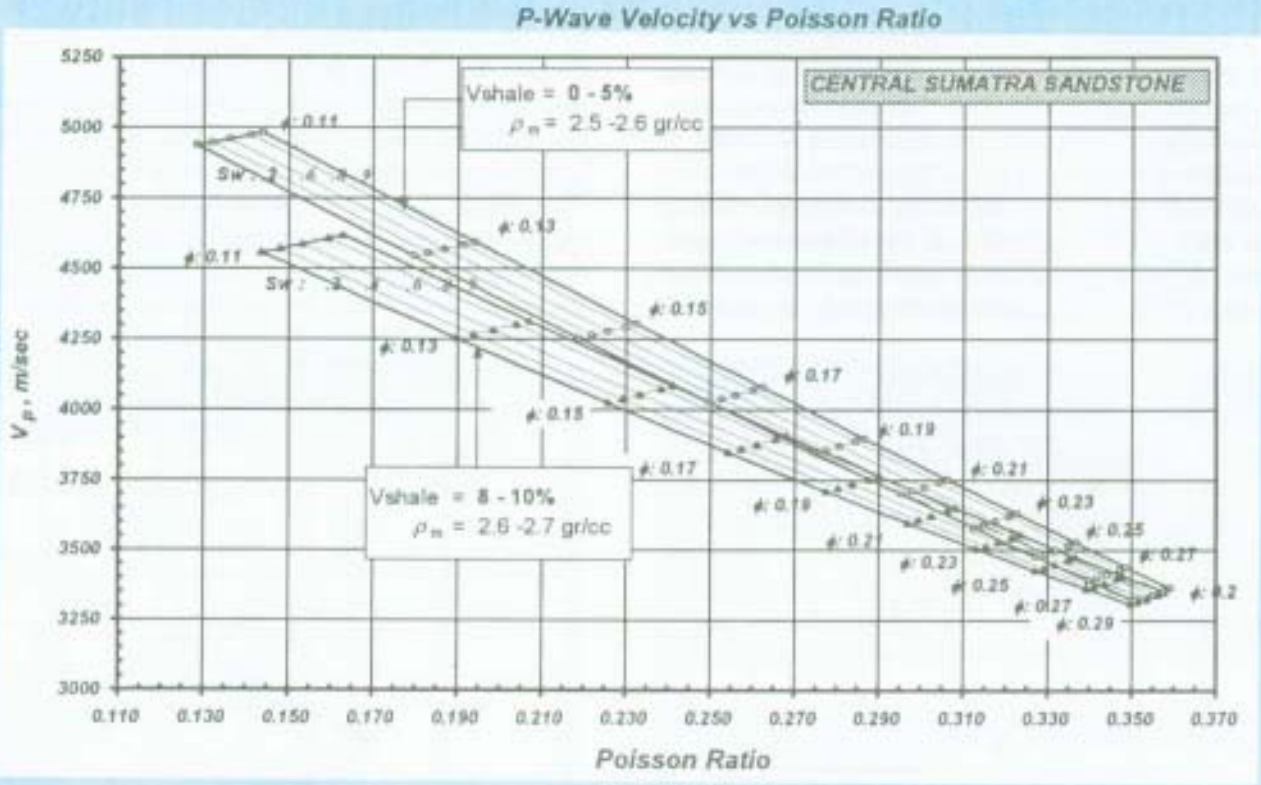

Figure 12
Examples of the resulting crossplots (in situ condition)
for the Central Sumatra sandstone, with acomodating effect of shaliness:
Vsh = 0 – 5 %, rm = 2.5 - 2.6 gr/cc and Vsh = 8 – 10 %, rm = 2.6 - 2.7 gr/c

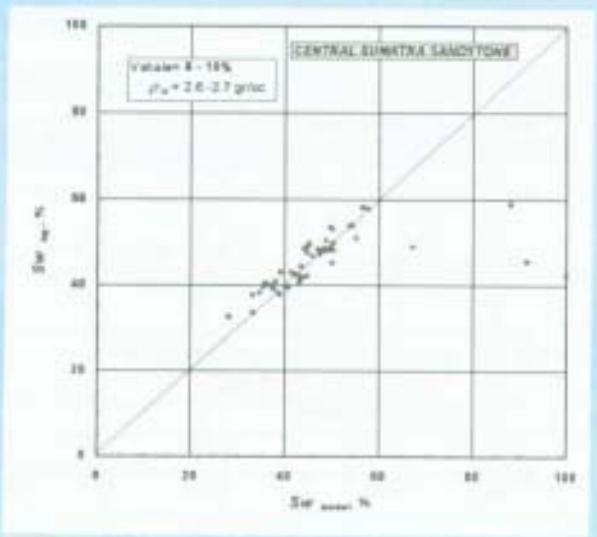

Figure 13a
Model validation through comparison of Poisson Ratio values after acomodating the effect of shaliness (Central Sumatra sandstone)
Vshale= 8 - 10 %, rm= 2.6 - 2.7 gr/cc

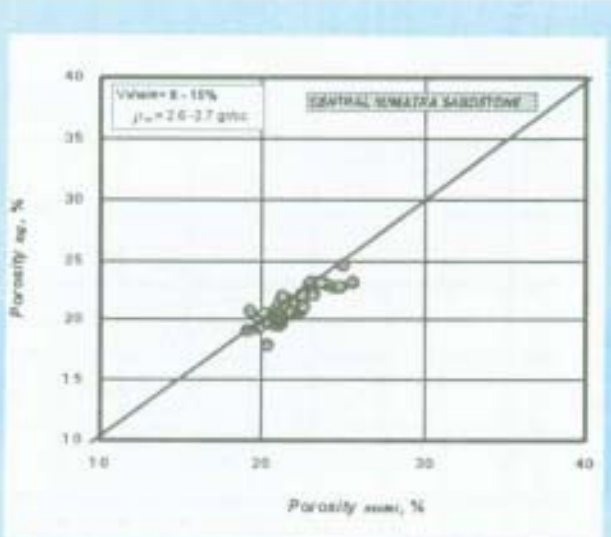

Figure 13b
Model Validation through comparison of Porosity after acomodating the effect of shaliness
(Central Sumatra sandstone)
Vshale= 8 - 10 %, rm=2.6 - 2.7 gr/cc

diminishing effect of shaliness on rocks with high porosity. Note that the V_{sh} values between the presented values are not plotted in order to provide a clear view on the division. Further analysis is made by plotting the V versus S_w for various porosity. Figure 8b is an example for data points represented by V_{sh} = 8 – 10 % ranges (examples are for porosity ranges of 19 – 20 % and 22 – 24 %). By similar plots for other V_{sh} ranges, there will be several plots similar to the one presented in Figure 8b. In conclusion, it is obvious that plots in Figure 8 have proved that the effect of shaliness

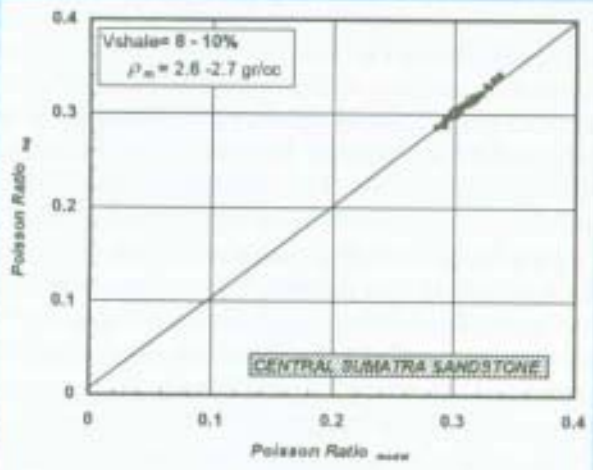

Figure 13c
Model validation through comparison of Poisson Ratio values after acomodating the effect of shaliness (Central Sumatra sandstone)
Vshale= 8 - 10 %, rm= 2.6 - 2.7 gr/cc

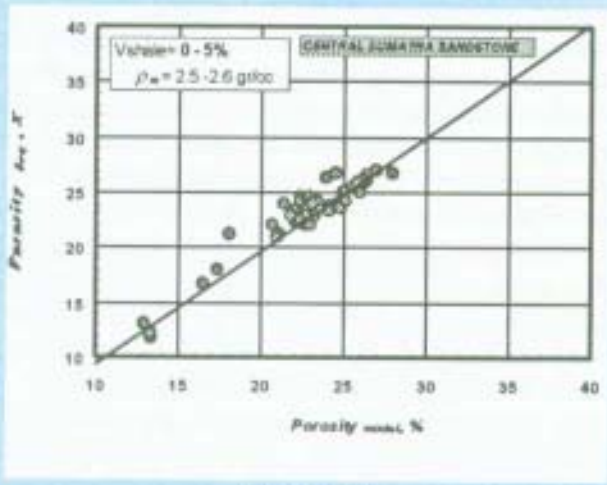

Figure 13e
Model Validation through comparison of Porosity after acomodating the effect of shaliness (Central Sumatra sandstone)
Vshale= 0 - 5 %, rm=2.5 - 2.6 gr/cc

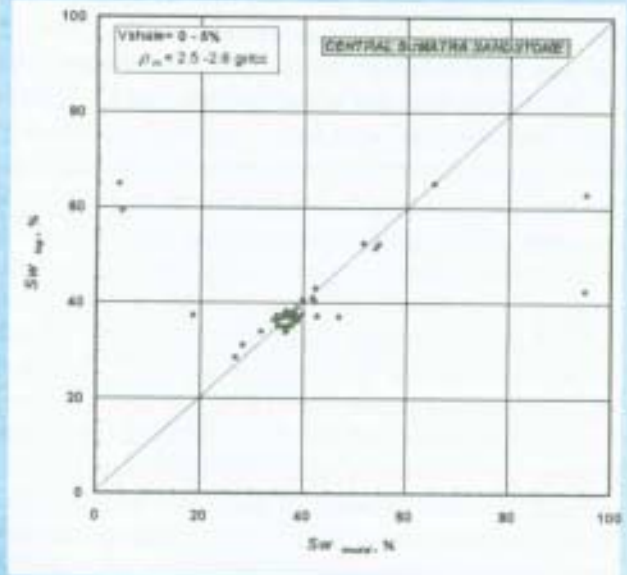

Figure 13d
Model validation through comparison of Poisson Ratio values after acomodating the effect of shaliness (Central Sumatra sandstone)
Vshale= 0 - 5 %, rm= 2.5 - 2.6 gr/cc

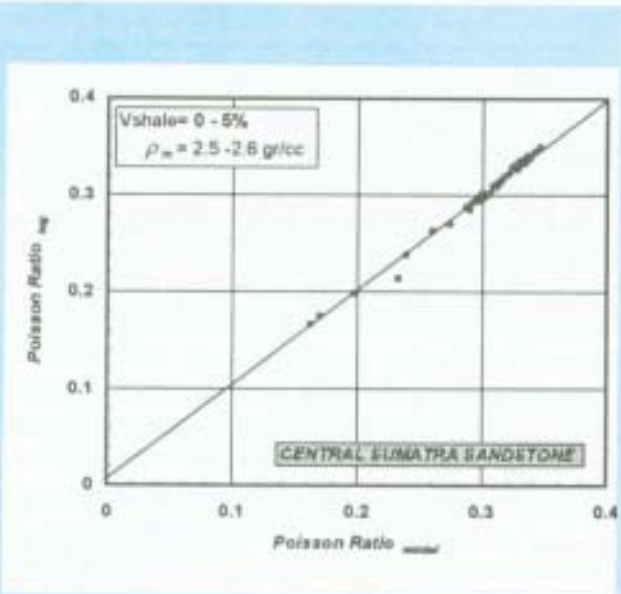

Figure 13f
Model validation through comparison of Poisson Ratio values after acomodating the effect of shaliness (Central Sumatra sandstone).
Vshale= 0 - 5 %, rm= 2.5 - 2.6 gr/cc

can be analyzed and later it will be proved that shale's scattering effect can be minimized.

The fact is rather different for the Natuna limestone. The same treatment was also given to the Natuna limestone. Plot between AI and porosity shown in Figure 9 does not give a clear separation between rocks with different matrix density. Further, Figure 10 also suggests that the clear division, based on V_{sh} ranges, shown by the Central Sumatra sandstone is not the case for the Natuna limestone. The plot otherwise exhibits not-so clear division. The complexity normally shown by limestone is probably the cause of the inconsistencies. Consequently, no further processes are given to the Natuna limestone.

The V_p - S_w plot, such as one in Figure 8b, is to facilitate the creation of new $V_{p,model} - V_{p,log}$ plots which will replace the one presented in Figure 3. By inputting pairs of predetermined porosity and water saturation values, V_p values from log ($V_{p,log}$) are determined using the the V_p - S_w plots. The same pairs were also used in determining the V_p from the crossplot, hence $V_{p,model}$, in Figure 2. The resulting $V_{p,model} - V_{p,log}$ plots, for r V_{sh} = 0 – 5 % and 8 – 10 %, are presented in Figures 11a and 11b respectively. It is obvious that the plot is substantially better compared to the "for all V_{sh} values" plot in Figure 3. This plot was then used for converting the crossplot in Figure 2 into *in situ* condition. Due to better data, this conversion is for the Central Sumatra sandstone only.

Following the same procedure, $V_{p,model} - V_{p,log}$ plots for other V_{sh} ranges were created using which any V_p values measured in laboratory ($V_{p,lab}$), as well as other properties (see Widarsono and Saptono, 1997), are converted to *in situ* condition. The resulting crossplots (for Vsh = 0 – 5 % and 8 – 10 %) are presented in Figure 12. Similar crossplots can also be created for other V_{sh} ranges. Thus, instead of having just one V_p-Poisson ratio-f-S_w crossplot the effort to establish a kind of correction on the presence of shaliness has resulted in a set of more reliable crossplots. The reliability is also exhibited by their relatively wider area covered by the two crossplots when compared to the crossplot in Figure 6a. With more crossplots representing other V_{sh} ranges the chance of having interpretable seismic data for determining porosity and S_w increases significantly.

In validating the crossplots, S_w values from the crossplot ($S_{w,model}$) are plotted against S_w values from log ($S_{w,log}$) for the same porosity values (figures in Figure 13 for both V_{sh} = 8 – 10 % and 0 – 5%). The validation process follows the same procedure as used previously. The validation plot proves itself better when compared to the plot in Figure 3, shown by the minimum data scatter. The evidence shown by the validation has enforced the need to analyze and correct the effect of shale presence. This also proves the approach taken in correcting the effect of shaliness works well, at least for the Central Sumatra sandstone.

V. FURTHER DISCUSSION

The different results shown by the two have pointed out two major concerns. The first is concerning the causes that have brought the difference. Considering matrix properties that contribute significantly to controlling the wave propagation, it is expected that differences in mineral composition and pore configuration play an important role. The shale presence in the Natuna reef is indeed minor when compared to the case of Central Sumatra sandstone. However, it is commonly acknowledged that reef limestones are often characterized by more complex pore systems and variation in stiffness (i.e. variation in bulk modulus, an elastic property that controls V_p) compared to normal sandstones. This certainly results in more irregularity in V_p when porosity and water saturation are taken as reference. The second concern is that even though shale presence in Natuna limestone is less, and probably surpassed by other factors, caution has to be taken when dealing with different shale in different rocks. Different shales are likely to affect the V_p-Poisson ratio-f-S_w crossplot in different ways. This is consistent with the commonly known difficulty to generalize the effect of shale on acoustic wave propagation. No attempts, however, are made to investigate more thoroughly the differences between the two shale, since it will not affect the overall conclusion significantly.

With the addition of accommodating shale presence, there are two additional steps that have to be added to the procedure proposed by Widarsono and Saptono (1997). If the main steps presented earlier in this paper are taken as the main steps, then the activities presented in Figures 7 and 8 are to be added after step 2. An improvement on the earlier proposed procedure has therefore been made. More thorough studies in aspects such as differences in shale types, frequency-related acoustic wave velocity dispersion, as well as more concentration on variation in lithology, can further be done in the future. This will produce a more reliable method for estimating water saturation and porosity throughout reservoir from seismic surveys. Having the above-mentioned factors been taken into consideration, it is very possible that the method will produce a significant number of V_p-Poisson ratio-f-S_w crossplots. This will certainly create a separate problem if the method is to be applied in real seismic data. In this case, a supporting method that facilitates pattern recognition, such as artificial neural network, is really required.

V. CONCLUSIONS

A set of conclusions that has been drawn from the work emphasizes:

1. With regard to porosity and water saturation, the presence of shale in sedimentary rocks tends to create inconsistencies and scatter in V_p. This is clearly proved by the results for Central Sumatra sandstone before the application of the new approach.
2. The presence of shale in rocks has to be analyzed and taken into consideration if a method for predicting water saturation and porosity from seismic survey is to be applied in the field.
3. The introduction of a set of V_p-Poisson ratio-f-S_w crossplots has increased the chance of having a larger quantity of interpretable V_p and Poisson ratio data obtained from seismic survey.
4. Different shale that are present either in the same or different sedimentary rocks has to be handled separately in order to accommodate their varied acoustic/elastic characteristics.
5. Although it is accepted that shale presence introduces complexity on acoustic wave velocities, hence the reliability of the proposed method, it is suspected that pore configuration and variation in matrix density could also play an important role.
6. The prospect of producing a relatively large number of V -Poisson ratio-f-S_w crossplots emphasizes the need to apply method that has the capability of pattern recognition, such as artificial neural network.

Acnowledgments

The authors woulk like to thank Mr. Tunggal from Formation Evaluation Group LEMIGAS and Mr. Hary Hardiman from LEMIGAS Core Laboratory for their kind and helpful assistance upon the completion of this work.

REFERENCES

1. **Biot, M.A.**, 1956, "Theory of Propagation of Elastic Waves in A Fluid-saturated Porous Solid. II. Higher Frequency Range", *J. Acoust. Soc. Am*, 28: 179-191.
2. **Domenico, S.N.**, 1976, "Effect of Brine-gas Mixture on Velocity in An Unconsolidated Sand Reservoir", *Geophysics*, 41: 882-894.
3. **Fjaer, E., Holt, R.M., Raaen, A.M.** and **Risnes, R.**, 1992, *Petroleum Related Rock Mechanics*, Elsevier Science Publishers BV, Amsterdam, p:338.
4. **Gassmann, F.**, 1951, "Elastic Waves Through a Packing of Spheres", *Geophysics*, 16: 673-685.
5. **Gregory, A.R.**, 1976, "Fluid Saturation Effects on Dynamic Elastic Properties of Sedimentary Rocks", *Geophysics*, 41: 895-924.
6. **Grim, R.E.**, 1968, *Clay Mineralogy*, McGraw-Hill Book company, 2nd ed-International Series in The Earth and Planetary Sciences, pp: 596.
7. **Hartley, K.B.**, 1981, "Factors Affecting Sandstone Acoustic Compressional Velocties and An Examination of Empirical Correlations Between Velocities and Porosities", *Trans. SPWLA*, paper PP.
8. **King, G.**, 1996a, "4-D Seismic Improves Reservoir Management Decisions. Part I", *World Oil*, March.
9. **King, G.**, 1996b, "4-D Seismic Improves Reservoir Management Decisions. Part II", *World Oil*, April.
10. **King, M.S.**, 1966, "Wave Velocities in Rocks as a Function of Changes in Overburden Pressure and Pore Fluid saturants", *Geophysics*, 31: 50-73.
11. **Koerperich, E.A.**, 1980, "Shear Wave Velocities Determined From Long- and Short-spaced Borehole Acoustic Devices", *Paper SPE* 8237.
12. **Kuster, G.T.** and **Tokzos, M.N.**, 1974, "Velocity and Attenuation of Seismic Waves in Two-phase Media: Part I: Theoretical Formulations", *Geophysics*, 39: 587 – 606.
13. **Minear, J.W.**, 1982, "Clay Models and Acoustic Velocities", *Paper SPE* 11031, presented at the 1982 SPE Annual Technical Conference and Exhibition, New Orleans.
14. **Timur, A.**, 1987, *Acoustic Logging*, in Petroleum Engineering Handbook by **H.W. Bradley** (editor-in-chief), Chapter 51, First printing, Society of Petroleum Engineer, Richardson, TX - USA.
15. **Widarsono, B.** and **Saptono, F.**, 1997, "Pengukuran Akustik di Laboratorium: Pendukung Dalam Perkiraan Porositas dan Saturasi Fluida Dari survei Seismik" (in Bahasa Indonesia). *Paper IATMI97-007*, Proceedings Simposium dan Kongres V IATMI, Jakarta.
16. **Widarsono, B.** and **Saptono, F.**, 1999, "Metoda Pemanfaatan Data pengukuran Akustik dan Log Sumur bagi penentuan porositas dan Saturasi Air dari Survei Seismik", *Submitted to Directorate General of Patent and Property Rights – Department of Justice – Republic of Indonesia*, Reg. no: P-990675 (19 July).

APPENDIX

Gassmann model for acoustic velocities in saturated porous medium (from Timur (1987)) can be expressed by:

$$V_p^2 = \frac{P_d + f(K_f)}{\rho_b} \qquad \text{(A-1)}$$

and

$$V_s^2 = \frac{G}{\rho_b} \qquad \text{(A-2)}$$

where P_d is the P-wave modulus for the rock frame (or dry

rock), and $f(K_f)$ is the function of the incompressibility of the fluid in the pore spaces. The P-wave modulus for the dry rock can be expressed, in turn, by:

$$P_d = K_d + \frac{4}{3}G_d \qquad \text{(A-3)}$$

and the function $f(K_f)$, by:

$$f(K_f) = K_f \frac{(1-\frac{K_d}{K_m})^2}{(1-\frac{K_f}{K_m})\phi + (K_m - K_d)\frac{K_f}{K_m^2}} \qquad \text{(A-4)}$$

in which K is incompressibility (or bulk modulus), G is shear modulus, and the subscript d, f, and m refer to the rock frame (or the dry rock,), fluid, and rock matrix.

For rock containing both water and hydrocarbon, the bulk density is expressed as:

$$\rho_b = \phi \cdot \rho_f + (1-\phi)\rho_m \qquad \text{(A-5)}$$

where:

$$\rho_f = S_w\rho_w + (1-S_w)\rho_{hc} \qquad \text{(A-6)}$$

and the fluid incompressibility, K_f, which is the inverse of compressibility, c_f, is given by:

$$K_f = \frac{1}{c_f} = \frac{1}{S_w c_w + (1-S_w)c_{hc}} \qquad \text{(A-7)}$$

where S denotes saturation, and the subscript hc refers to hydrocarbon.

Rock frame incompressibility, K_d, in Equation A-3, which is the inverse of compressibility of dry rock, c_d, is related to PV compressibility, c_p, by:

$$K_d = \frac{1}{c_d} = \frac{1}{\phi \cdot c_p + c_m} \qquad \text{(A-8)}$$

By knowing V_p and V_s in fluid saturated rock as well as in the dry rock, the Poisson ratio, n, can be calculated through the use of

$$\nu = \frac{\left(V_p/V_s\right)^2 - 2}{2\left(V_p/V_s\right)^2 - 2} \qquad \text{(A-9)}$$